© 2015. Published by The Company of Biologists Ltd | Development (2015) 142, 1745-1755 doi:10.1242/dev.121434

RESEARCH ARTICLE

STEM CELLS AND REGENERATION

CSR-1 and P granules suppress sperm-specific transcription in the *C. elegans* germline

Anne C. Campbell and Dustin L. Updike*

ABSTRACT

Germ granules (P granules) in *C. elegans* are required for fertility and function to maintain germ cell identity and pluripotency. Sterility in the absence of P granules is often accompanied by the misexpression of soma-specific proteins and the initiation of somatic differentiation in germ cells. To investigate whether this is caused by the accumulation of somatic transcripts, we performed mRNA-seq on dissected germlines with and without P granules. Strikingly, we found that somatic transcripts do not increase in the young adult germline when P granules are impaired. Instead, we found that impairing P granules causes sperm-specific mRNAs to become highly overexpressed. This includes the accumulation of major sperm protein (MSP) transcripts in germ cells, a phenotype that is suppressed by feminization of the germline. A core component of P granules, the endo-siRNA-binding Argonaute protein CSR-1, has recently been ascribed with the ability to license transcripts for germline expression. However, impairing CSR-1 has very little effect on the accumulation of its mRNA targets. Instead, we found that CSR-1 functions with P granules to prevent MSP and sperm-specific mRNAs from being transcribed in the hermaphrodite germline. These findings suggest that P granules protect germline integrity through two different mechanisms, by (1) preventing the inappropriate expression of somatic proteins at the level of translational regulation, and by (2) functioning with CSR-1 to limit the domain of sperm-specific expression at the level of transcription.

KEY WORDS: *C. elegans*, P granules, CSR-1, Germ granules, Germline, Sperm, Spermatogenesis, Germline sex determination

INTRODUCTION

Germ cells are pluripotent and immortal. These properties are maintained through extrinsic signals from the germline stem cell niche, as well as through intrinsic signals originating from both the nucleus and cytoplasm. In the cytoplasm, non-membrane-bound organelles called germ granules are found in germ cells across phyla. In some species, their presence can induce soma to develop as germline, suggesting that germ granules function to promote cellular pluripotency (Illmensee and Mahowald, 1974; Tada et al., 2012).

In *C. elegans*, germ granules are called P granules (Strome and Wood, 1982). In the adult germline, they act to maintain totipotency by repressing somatic cell fate via an unknown mechanism. Most P-granule-associated proteins identified to date contain RNA-binding domains or are known regulators of translation, suggesting that P granules act post-transcriptionally to maintain germline pluripotency [reviewed by Sengupta and Boag (2012)]. When P granules are impaired in the adult germline, germ cells lose pluripotency, and a fraction initiate somatic reprogramming (Updike et al., 2014). The mechanisms behind the ability of P granules to maintain pluripotency by repressing somatic fate are currently not understood. One model is that P granules create a microenvironment in which nascent transcripts can be surveyed as they exit the nucleus, and those not licensed for germline expression can be selectively silenced (Kasper et al., 2013; Sheth et al., 2010; Updike et al., 2011). These transcripts include foreign and viral mRNAs that could compromise genome stability, as well as transcripts encoding somatic differentiation factors that might be stochastically expressed in the germline. If this model is correct, silenced expression of these transcripts could be accomplished either at the level of translation or at the level of transcript accumulation. If by translation, it implies that somatic mRNAs are already present in the germline, either at low levels or through stochastic expression in a subset of germlines, and that they need not be elevated to express somatic proteins when P granules are impaired. If by transcript accumulation, somatic mRNAs will be elevated in P-granule-depleted germlines, either through increased transcription of somatic mRNAs or through increased somatic mRNA stabilization. Microarray expression profiles in mutants lacking core P-granule components (i.e. DEPS-1 and GLH-1) have shown surprisingly few changes when compared with wild-type worms, supporting a model for translational regulation as opposed to the accumulation and/or degradation of mRNA (Spike et al., 2008a,b). However, these expression profiles have been limited to single mutants in gene families, and in fertile worms that do not completely disrupt P-granule assembly. To fully understand how P granules regulate mRNA, transcript accumulation needs to be analyzed in dissected germlines in the presence and absence of P granules.

In *C. elegans*, germline expression is primarily regulated post-transcriptionally through 3′ UTR binding proteins. An exception is sperm-specific transcription, which instead depends on promoter sequences (Kulkarni et al., 2012; Merritt et al., 2008; Shim, 1999). In the fourth larval stage (L4), ~40 germ cells in each of the gonad arms of the hermaphrodite undergo spermatogenesis and develop into 160 spermatids [reviewed by Chu and Shakes (2013)]. Mature sperm are then stored in spermathecae and used to fertilize the remaining germ cells that develop into oocytes. During the process of spermatogenesis, P granules are disassembled [reviewed by Updike and Strome (2010), figure 2]. First, the P-granule nucleating factors PGL-1 and PGL-3 are cleared from P-granules so that they are not present in secondary spermatocytes (Amiri et al., 2001; Kawasaki et al., 1998, 2004). At the same time, two endo-siRNA-binding Argonaute proteins, ALG-3 and ALG-4, become expressed and overlap with PGL-1/3 expression in primary spermatocytes, but persist in secondary spermatocytes after PGLs are cleared (Conine

Kathryn W. Davis Center for Regenerative Biology and Medicine, Mount Desert Island Biological Laboratory, Bar Harbor, ME 04672, USA.

*Author for correspondence (dupdike@mdibl.org)

Received 22 December 2014; Accepted 19 March 2015

Development (2015) 142, 1745-1755 doi:10.1242/dev.121434

et al., 2013). ALG-3 and ALG-4, along with other constitutive P-granule components, including the mRNA cap-binding translation factor IFE-1 and the Vasa homologs GLH-1 and GLH-4, remain localized to P granules in secondary spermatocytes until remaining P-granule components disassemble and are deposited in residual bodies during spermatid budding (Amiri et al., 2001; Conine et al., 2010; Gruidl et al., 1996). This small time window, when PGL-1/3 begins to be cleared from P granules in primary spermatocytes until spermatid budding, coincides with the onset of transcription and subsequent translation of sperm-specific mRNAs. IFE-1, which facilitates this sperm-specific translation (Henderson et al., 2009; Kawasaki et al., 2011), physically interacts with PGL-1 (Amiri et al., 2001). This interaction is predicted to repress IFE-1 activity until PGL-1 is cleared from P granules at the onset of spermatogenesis (Amiri et al., 2001). PGL-1 clearing might also be required to initiate *alg-3* and *alg-4* transcription. Once expressed, ALG-3 and ALG-4 bind to endo-siRNAs (26Gs) that complement sperm-specific transcripts, but it is unclear whether these two Argonaute proteins degrade or protect their mRNA substrates (Conine et al., 2010, 2013; Han et al., 2009; Pavelec et al., 2009). Once sperm-specific genes are transcribed and translated, their proteins are packaged into transcriptionally and translationally silent spermatids.

A core component of P granules called CSR-1 is essential for proper spermatogenesis and germline expression. CSR-1 is an endogenous siRNA-binding Argonaute protein that specifically binds tri-phosphorylated 22-basepair endo-siRNAs (22Gs) that are complementary to germline-expressed transcripts (Claycomb et al., 2009). In adult hermaphrodites, CSR-1 22Gs do not target sperm-specific transcripts, but in males they do (Conine et al., 2013). A number of recent publications have shown that CSR-1 retains an epigenetic memory of germline expression from one generation to the next, and might function to license mRNAs for germline expression (Cecere et al., 2014; Conine et al., 2013; Gu et al., 2009; Lee et al., 2012; Seth et al., 2013; Shirayama et al., 2012; Wedeles et al., 2013). This ability probably ensures that somatic and foreign transcripts (those not licensed for germline expression) are either degraded or silenced within P granules [reviewed by Kasper et al. (2013)]. RNAi depletion of *csr-1* (and its co-factors *ekl-1*, *drh-3* and *ego-1*) causes a very specific, large P-granule phenotype and cytoplasmic pooling of RNA (Claycomb et al., 2009; Updike and Strome, 2009; Vought et al., 2005). Together, these findings suggest that P-granule and CSR-1 functions are tightly integrated in maintaining germline integrity.

Here, we examine the expression profile of *C. elegans* germlines that have been depleted of P granules, and compare this with the expression profile of *csr-1*-depleted germlines. Our findings suggest that translational regulation, and not mRNA accumulation/degradation, is the mechanism used to silence aberrant somatic transcripts and preserve germline pluripotency. Strikingly, we also find that P granules and CSR-1 both function to suppress sperm-specific transcription and masculinization in *C. elegans* hermaphrodites by regulating the germline sex determination pathway.

RESULTS

Expression in P-granule-depleted germlines

We previously demonstrated that impairing P granules causes the loss of germ-cell pluripotency. This is accompanied by a small fraction of P-granule-depleted germlines that express muscle-specific and pan-neuronal markers in germ cells (Updike et al., 2014). One possible mechanism to explain these germ cell reprogramming events is that P granules function to repress the accumulation of somatic transcripts that become stochastically transcribed in the germline. To test this, we performed both control (empty vector RNAi) and P-granule RNAi by simultaneously targeting four core P-granule components (PGL-1, PGL-3, GLH-1 and GLH-4) as previously described (Updike et al., 2014). We then prepared total RNA from *C. elegans* germlines dissected from young adult hermaphrodites (animals with a vulva, one day following the fourth larval stage, see supplementary material Fig. S1). Four biological replicates for each condition, consisting of ∼500 dissected germlines each, were obtained and prepared for mRNA-seq. Using the pipeline described in the Materials and Methods, we identified transcripts in the germline corresponding to 14,390 out of 20,259 annotated coding genes (WBcel215), each represented anywhere from a normalized average of 1 to 435,500 sequences (Fig. 1A; supplementary material Table S1, column D). We compared our data with germline- and soma-enriched datasets (Reinke et al., 2004), and found that 95% of previously defined germline-enriched genes were represented by our set of 14,390, with an average of 3002 sequences per gene. We also found that 88% of previously defined soma-enriched genes were represented in our set of 14,390, with an average of 680 sequences per gene. Next, we compared our list of germline-expressed genes with compiled germline- and soma-specific datasets (Rechtsteiner et al., 2010), and found all previously defined germline-specific genes present in our dataset, with an average of 5424 sequences per gene. Ninety-four percent of soma-specific genes were also represented, with an average of 861 sequences per gene. As dissected germlines contain somatic gonad cells, they are a potential source for these soma-specific transcripts; however, single-molecule fluorescent *in situ* hybridization (smFISH) of two 'soma-specific' transcripts, *unc-16* and *hbl-1*, exhibited foci on the periphery of pachytene nuclei (supplementary material Fig. S2). Together, these results show that many traditionally defined soma-enriched and soma-specific genes might still be transcribed in the germline, suggesting a need for germline components that actively inhibit their translation to prevent germ-to-soma reprogramming.

Following P-granule RNAi, we observed 1149 genes with a *P*-value <0.05 that corresponds to at least a twofold change in transcript accumulation over the control (1043 up and 106 down), and we refer to this as 'set 1' (Fig. 1A; supplementary material Table S1, column I). To reduce false positives, we used an adjusted *P*-value <0.05, corresponding to at least a 3.6-fold change, to obtain a more stringent list of 102 genes, which we refer to as 'set 2' (supplementary material Table S1, column J). P-granule RNAi decreased transcripts from the target genes (*pgl-1*, *pgl-3*, *glh-1* and *glh-4*) by a fold change of 9.4, 6.3, 1.5 and 4.7, respectively, and resulted in over 80% sterility in each of the replicates. To test the hypothesis that P-granule depletion causes increased accumulation of somatic transcripts, we compared our P-granule RNAi dataset with both germline- and soma-enriched datasets defined previously (Reinke et al., 2004) (Fig. 1B). Germline-enriched genes exhibited a slight but significant increase in transcript levels, whereas soma-enriched genes showed no change. We also did not observe increased transcripts from a previously defined set of neuronal genes (Watson et al., 2008), despite our previous observation that continuing P-granule RNAi for one day longer causes ∼10% of sterile germlines to express pan-neuronal markers (Updike et al., 2014). In fact, of the 5867 genes not expressed, only 45 (0.77%) showed a significant increase in transcripts after P-granule RNAi (3.9% of set 1), which is 7.4-fold lower than expected by chance (Fig. 1A, left, *P*=4E-103). Likewise, of the 5867 most abundantly expressed genes, only 47 showed a significant change in transcript

Development (2015) 142, 1745-1755 doi:10.1242/dev.121434

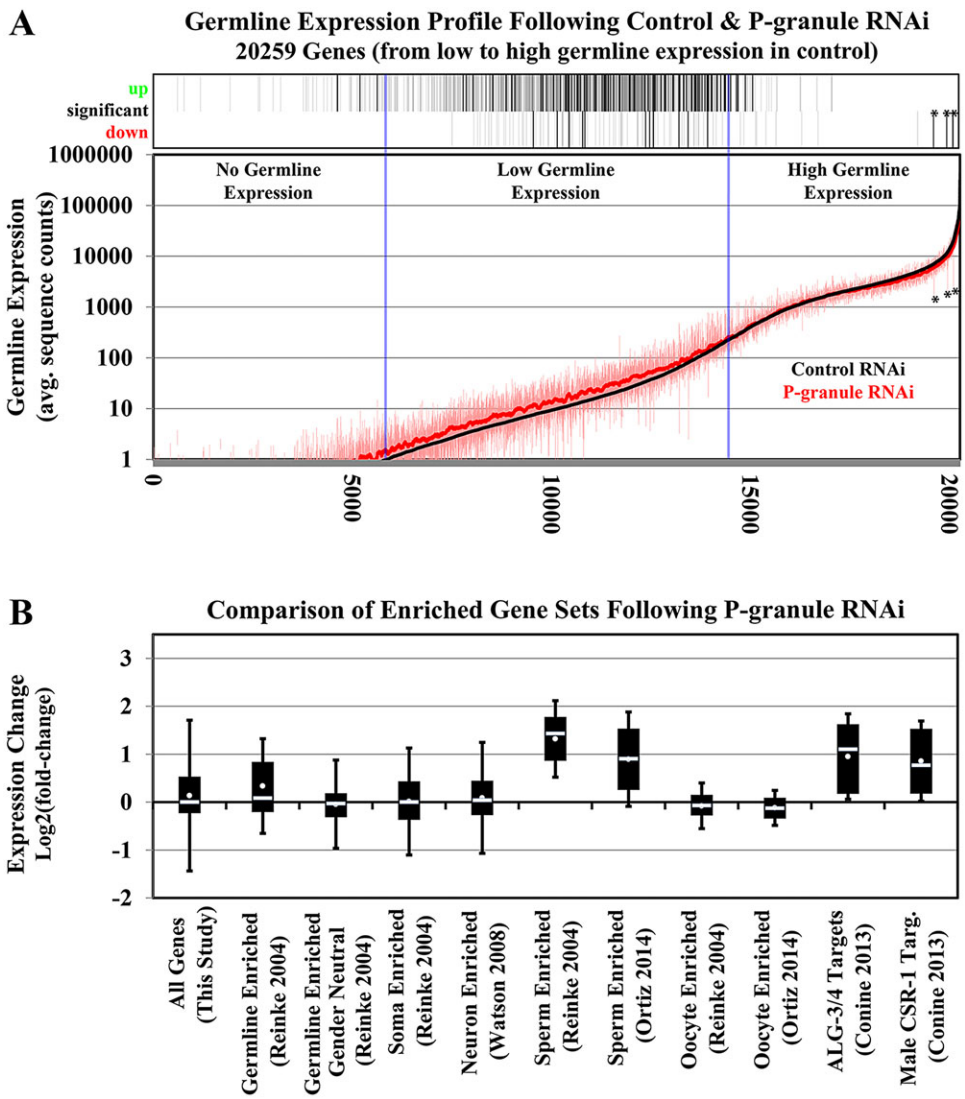

Fig. 1. Comparison of wild-type and P-granule RNAi expression profiles. (A) Average germline expression of genes following control (black line) and P-granule (pink-red line, running average) RNAi (log scale). Genes are ranked from low to high expression based on the control RNAi dataset. Top box shows position of genes significantly up- or downregulated by P-granule RNAi. *RNAi targets (*glh-4*, *pgl-3* and *pgl-1*, respectively). (B) Comparison of expression changes following P-granule RNAi in published enriched gene datasets (see supplementary material Table S1). Box, upper and lower quartiles; line, median; dots, mean; bars, s.d.

levels (Fig. 1A, right, *P*=3E-101). The remaining genes from set 1 are transcribed and accumulate at very low levels in dissected germlines (represented by an average of only 1 to 213 sequences in our mRNA-seq data; Fig. 1A, center). These 'low germline expression' genes show a slight increase in transcript accumulation when P granules are impaired. However, we conclude that P granules have very little effect on the mRNA accumulation of abundantly expressed germline genes or on transcripts that do not accumulate in the germline. This suggests that, if P granules repress the expression of somatic transcripts, as we hypothesize, such regulation must occur at the level of translation and not mRNA accumulation/degradation.

P granules function to repress sperm-specific mRNA accumulation in the hermaphrodite germline

Gene ontology analysis of upregulated set 1 genes following P-granule RNAi shows an enrichment in terms associated with spermatogenesis. We therefore compared upregulated set 1 genes with available gamete-enriched datasets (Chu et al., 2006; Ortiz et al., 2014; Reinke et al., 2004). We found that oocyte-enriched genes are slightly downregulated, whereas sperm-enriched genes are highly upregulated following P-granule RNAi (Fig. 1B). In fact, 81% (848/1043) of upregulated P-granule RNAi set 1 genes are in at least one of the sperm-enriched datasets, and this increases to 87% (76/87) in more stringent set 2 genes (supplementary material Table S1, column X). Subtracting sperm- and oocyte-specific genes from the germline-enriched dataset demonstrated that the increased transcript accumulation of germline-enriched genes following P-granule RNAi can be attributed entirely to the presence of sperm-enriched genes (Fig. 1B; supplementary material Table S1, column R). Genes upregulated by P-granule RNAi encode several major sperm proteins (MSPs), the sperm-specific PP1 phosphatases GSP-3 and GSP-4, other sperm-specific chromatin factors, including HTAS-1, SPCH-1, SPCH-2, SPCH-3, SPE-11, SMZ-1 and SMZ-2, and the sperm-specific small RNA-binding Argonautes ALG-3 and ALG-4 (supplementary material Table S1). mRNAs from these latter two genes increase 2.2- and 2.4-fold after P-granule RNAi. Interestingly, genes regulated by P granules do not include those encoding SPE-44 and ELT-1, which have been shown to promote sperm-specific transcription (Kulkarni et al., 2012; Shim, 1999), or IFE-1, which promotes sperm-specific translation (Kawasaki et al., 2011).

Expression in *csr-1*-depleted germlines

The core P-granule component CSR-1 has been ascribed with the ability to distinguish between transcripts that should be expressed in the germline and those that should not (Seth et al., 2013; Wedeles

Development (2015) 142, 1745-1755 doi:10.1242/dev.121434

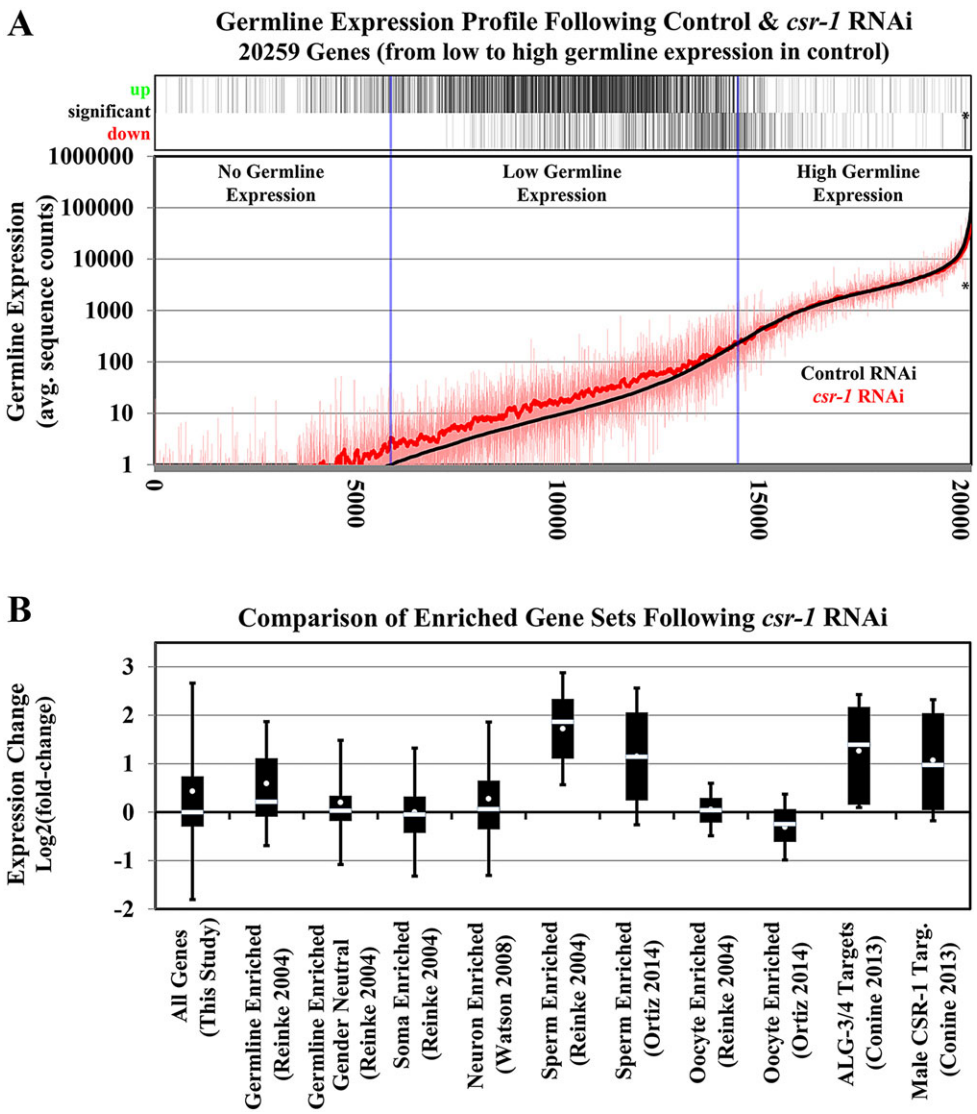

Fig. 2. Comparison of wild-type and *csr-1* RNAi expression profiles. (A) Average germline expression of genes following control (black line) and *csr-1* (pink-red line, running average) RNAi (log scale). Genes are ranked from low to high expression, based on the control RNAi dataset. Top box shows position of genes significantly up- or downregulated by *csr-1* RNAi. *RNAi target RNAi (*csr-1*). (B) Comparison of expression changes following *csr-1* RNAi in published enriched gene datasets (see supplementary material Table S1). Box, upper and lower quartiles; line, median; dots, mean; bars, s.d.

et al., 2014). In addition, CSR-1 is required for proper spermatogenesis in *C. elegans* males (Conine et al., 2013). In light of this, we also wanted to examine germline expression profile following the loss of *csr-1*. Microarray and Gro-seq expression profiles have previously been performed in *csr-1* whole worms (Cecere et al., 2014; Claycomb et al., 2009). To examine germline-specific expression, we performed *csr-1* RNAi and dissected germlines from young adult hermaphrodites. This was also carried out with four biological replicates consisting of ~500 dissected germlines each. Correlation between germline mRNA-seq following *csr-1* RNAi and previously performed microarray tiling profiles in a *csr-1* mutant (Claycomb et al., 2009) was strong between transcripts that increased more than twofold (supplementary material Fig. S3A, B). Downregulated genes on the tiling arrays showed no change in transcript accumulation with *csr-1*(RNAi) mRNA-seq. One notable difference, because we sequenced mRNA and not total RNA, is that we were unable to detect a decrease in histone mRNA levels following *csr-1* RNAi as previously reported (Avgousti et al., 2012). Previous findings (Claycomb et al., 2009) in hermaphrodites, suggesting that the loss of CSR-1 primarily affects the accumulation of non-CSR-1 target mRNAs (i.e. mRNAs not targeted by 22G siRNAs bound to CSR-1), were supported by our results (supplementary material Fig. S3B). We observed 2327 significantly regulated genes in germlines following *csr-1* RNAi, with a *P*-value <0.05, corresponding to a fold change >1.9 (Fig. 2A; supplementary material Table S1, column O). An adjusted *P*-value <0.05 was calculated to obtain a more stringent list of 949 genes, corresponding to a fold change >2.6 (supplementary material Table S1, column P). Of the significantly regulated genes, only 4% of set 1 and 5% of set 2 were previously shown to complement CSR-1-bound 22G siRNAs (Claycomb et al., 2009), a percentage fivefold (set 1) and 18-fold (set 2) lower than expected by chance. Both *glh-1* and *glh-4* fall into this group of CSR-1 targets that are upregulated (2.6- and 2.3-fold, respectively) with *csr-1* RNAi. This result was similar to what we previously reported by qRT-PCR (Updike and Strome, 2009), suggesting that CSR-1 negatively modulates transcript levels of core P-granule components. Increased expression of *glh-1* and *glh-4*, although modest, might contribute to the large P-granule phenotype that is observed in germlines when *csr-1* is depleted.

CSR-1 also functions to repress sperm-specific mRNA accumulation in the hermaphrodite germline

Strikingly, both *csr-1* RNAi and P-granule RNAi expression profiles showed a high degree of correlation (Fig. 3;

Development (2015) 142, 1745-1755 doi:10.1242/dev.121434

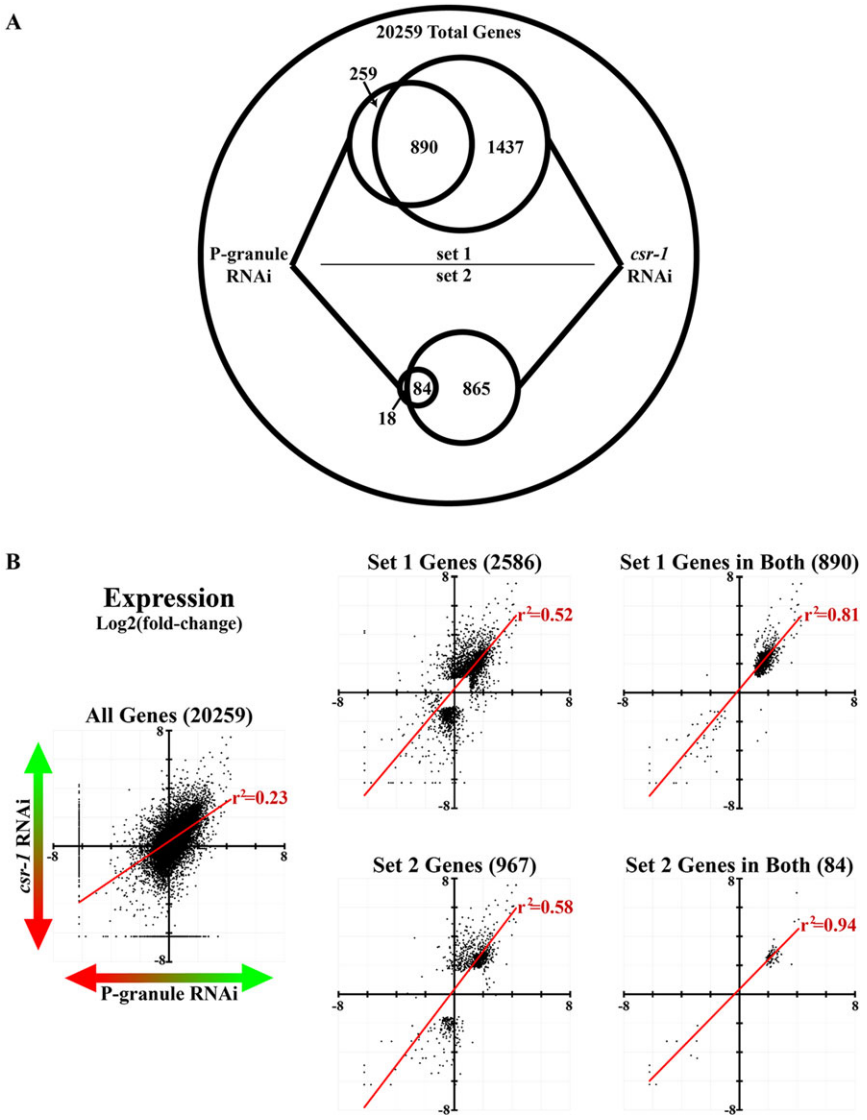

Fig. 3. Correlation of germline expression changes between P-granule and *csr-1*-depleted worms. (A) Proportional Venn diagram comparing both set 1 (less stringent) and set 2 (highly stringent) datasets from *csr-1* and P-granule RNAi experiments. (B) Correlation plots comparing *csr-1* and P-granule RNAi log2 fold changes.

supplementary material Table S1). We compared *csr-1*(RNAi) upregulated genes with available gamete-enriched datasets (Chu et al., 2006; Ortiz et al., 2014; Reinke et al., 2004). As with P-granule RNAi, we found that oocyte-enriched genes are slightly downregulated, whereas sperm-enriched genes are highly upregulated following *csr-1* RNAi (Fig. 2B). Of upregulated *csr-1* RNAi set 1 genes, 59% (1044/1760) are sperm-enriched, increasing to 68% (533/781) in set 2 genes (supplementary material Table S1, column X). Increased transcript accumulation of germline-enriched genes following *csr-1* RNAi can also be attributed entirely to the presence of sperm-enriched genes (Fig. 2B; supplementary material Table S1, column R). Again, these upregulated genes encode several MSPs, the sperm-specific PP1 phosphatases GSP-3 and GSP-4, other sperm-specific chromatin factors, including HTAS-1, SPCH-1, SPCH-2, SPCH-3, SPE-11, SMZ-1 and SMZ-2, and genes encoding ALG-3 and ALG-4, which are upregulated 2.9- and 3.1-fold, respectively (supplementary material Table S1). SPE-44 and IFE-1 are also not differentially expressed. These results suggest that the functions of P granules and CSR-1 are tightly integrated.

Argonaute proteins, such as CSR-1, ALG-3 and ALG-4, are directed to their mRNA substrates through sequence-specific small RNAs. CSR-1-bound 22G siRNAs selectively target germline-expressed transcripts, whereas ALG-3/4 26G siRNAs selectively target sperm-specific transcripts (Conine et al., 2010). CSR-1 has recently been shown to act in the ALG-3/4 pathway to promote male spermatogenesis (Conine et al., 2013). In the hermaphrodite germline, however, our results showed that CSR-1 negatively regulates the expression of sperm-specific genes. This might reflect distinct gender roles for CSR-1, depending on whether ALG-3 and ALG-4 are present. In an *alg-4; alg-3* double mutant, ALG-3/4 mRNA targets exhibit very little change in accumulation (Conine et al., 2013). By contrast, 45% (634/1403) of ALG-3/4 targets are significantly regulated, all positively, following P-granule RNAi (set 1), and the average expression of all ALG-3/4 targets is significantly increased (Fig. 1B). Likewise, 51% (721/1405) of ALG-3/4 targets are significantly regulated, 719/721 positively, following *csr-1* RNAi (set 1), and the average expression of all ALG-3/4 targets is also significantly increased (Fig. 2B). One possible model is that, instead of regulating targets with bound 22G siRNAs, CSR-1 functions in conjunction with P granules to repress *alg-3/4* transcription and ALG-3/4 target gene expression in the germline of adult hermaphrodites. CSR-1 was previously found to bind 22G siRNAs corresponding to sperm-specific genes in males;

Development (2015) 142, 1745-1755 doi:10.1242/dev.121434

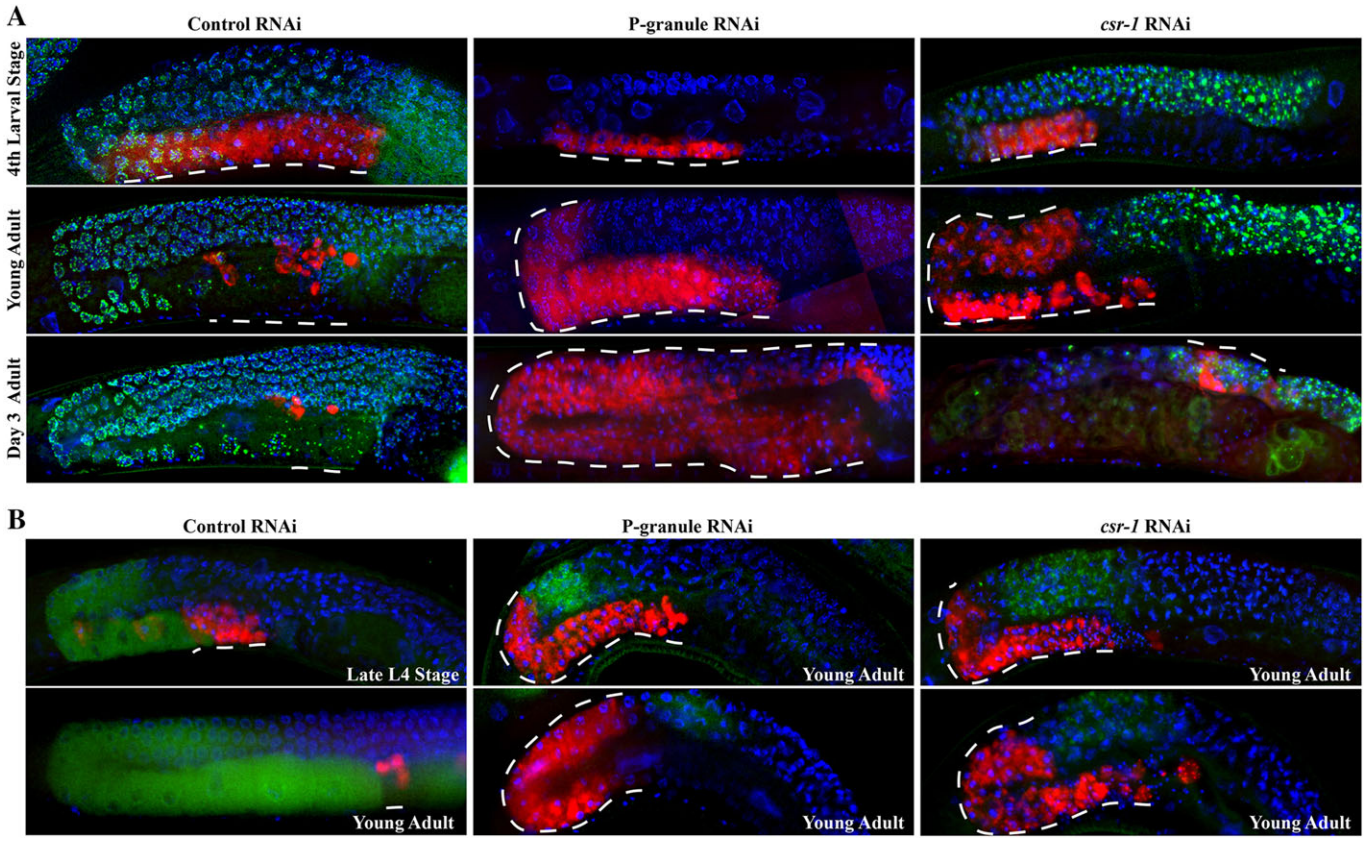

Fig. 4. Distal expansion of *msp-3* expression following P-granule and *csr-1* RNAi. (A) Representative images show the left gonad arm in fixed whole worms at L4, young adult and day 3 adult stages. Expansion of *msp-3* expression is observed following either P-granule or *csr-1* RNAi. (B) *msp-3* expansion (red) following P-granule or *csr-1* RNAi pushes back or suppresses the expression of LIN-41::GFP, an early marker of oocyte development. Red, *msp-3* FISH probe; blue, DAPI/DNA; green, PGL-1::GFP in A and LIN-41::GFP in B. Dashed lines indicate domain of *msp-3* expression.

however, these sperm-mRNA-targeting 22Gs are not present in adult hermaphrodites (Conine et al., 2013). Interestingly enough, we observed that male-specific CSR-1 mRNA targets are significantly upregulated following either *csr-1* or P-granule RNAi in the germlines of adult hermaphrodites (Fig. 1B and Fig. 2B). Our findings suggest that the ability of CSR-1 to repress sperm-specific mRNA accumulation in adult hermaphrodites might be indirect and/or independent of the subset of CSR-1-bound 22Gs that directly bind sperm-specific transcripts in males, and further testing is warranted to determine whether that is the case.

CSR-1 and multiple P-granule components inhibit sperm mRNA expression

In order to visualize, and thereby verify, the accumulation of sperm-specific mRNA following either P-granule or *csr-1* RNAi, we performed FISH on *msp-3* transcripts in whole-mounted worms. Under control RNAi conditions, *msp-3* becomes expressed in the L4 stage in the most proximal germ cells that undergo spermatogenesis. In young adult and 3-day-old adult worms, *msp-3* transcripts are only detected in a handful of residual bodies that remain after the completion of spermatogenesis (Fig. 4A; Table 1). After depleting P granules or *csr-1* with RNAi, the domain of *msp-3* expression expands past the bend in the gonad in young adults, and in 3-day-old adults can even reach the distal end of the germline. We found that 16% of worms show a distal expansion of *msp-3* in young adults following P-granule RNAi, whereas this expansion is observed in 35% of young adults following *csr-1* RNAi (Fig. 4A; Table 1). Similar distal expansions were observed for the sperm-enriched transcripts *ssq-1* and *rmd-3* (supplementary material Fig. S4). As was previously described, P-granule RNAi causes premature cellularization of germ cells (Updike et al., 2014). These *msp-3*$^{+}$ cells do not express LIN-41::GFP, a marker of maturing oocytes, and in *csr-1*- and P-granule-depleted worms, the domain of LIN-41::GFP expression is retracted or absent depending on the extent of *msp-3* expression (Fig. 4B). This suggests that proximal germ cells that would otherwise develop as oocytes now initiate spermatogenesis when *csr-1* or P granules are impaired. However, this germline masculinization phenotype is incomplete, as these cells in young adults and 3-day-old adults do not stain with an antibody (SP56) that recognizes epitopes in mature spermatids (data not shown). The expansion of *msp-3* provides convincing evidence that a primary role of P granules, possibly through CSR-1, might be to limit the extent of germ cells that initiate spermatogenesis in the developing hermaphrodite by promoting the switch from spermatogenesis to oogenesis. The presence of a vulva (supplementary material Figs S5 and S6, arrowheads), the position of the distal end of the germline, and the expansion of *msp-3* in 3-day-old adults suggests that this phenotype is not due to delayed germline development. This suggests that P-granule components actively suppress germline masculinization to promote proper germ cell and oocyte development.

Next, we wanted to determine whether the expansion of *msp-3* expression is caused by compromised P granules or by the loss of specific P-granule components. This is always a difficult question to resolve, as P-granule integrity can be compromised by impairing a number of individual P-granule components. Single mutations in all

Development (2015) 142, 1745-1755 doi:10.1242/dev.121434

Table 1. *msp-3* mRNA expansion and suppression

	Control RNAi		P-granule RNAi		*pgl-1; pgl-3* RNAi		*pgl-1* RNAi		*glh-1* RNAi		*csr-1* RNAi	
Wild-type N2	0/204	0%	11/70	16%*	36/181	20%*	21/117	18%*	9/30	30%*	45/129	35%*
pgl-1(bn101); pgl-3(bn104)	0/37	0%	–	–	–	–	–	–	–	–	–	–
glh-4(gk224) glh-1(ok439)	20/109	18%*	–	–	–	–	–	–	–	–	–	–
pgl-1(bn101)	48/157	31%*	–	–	–	–	–	–	–	–	77/232	33%*
pgl-3(bn104)	21/103	20%*	–	–	–	–	–	–	–	–	116/179	65%*
ife-1(bn127)	0/79	0%	19/249	8%*	19/87	22%*	–	–	–	–	13/136	10%*
alg-4(ok1041); alg-3(tm1155)	7/190	4%	12/69	17%*	75/306	25%*	–	–	–	–	77/115	67%*
fog-3(q470)/+	0/28	0%	25/85	29%*	11/37	30%*	–	–	–	–	–	–
fog-3(q470)	0/99	0%	0/36	0%	0/24	0%	–	–	–	–	0/56	0%
fem-3(e2006)	0/200	0%	0/200	0%	0/200	0%	–	–	–	–	–	–

Table shows the number of young adult worms scored and the percentage exhibiting a distal expansion of *msp-3* FISH signal past the ventral to dorsal bend of the germline. *P<0.0005.

four of our core target genes (*pgl-1*, *pgl-3*, *glh-1* and *glh-4*) caused P-granule defects, but not the complete removal of P granules. We found that simultaneous RNAi depletion of the redundantly functioning paralogs *pgl-1* and *pgl-3* (Kawasaki et al., 2004) caused *msp-3* expansion in 20% of worms (supplementary material Fig. S5; Table 1). This expansion was also observed in 18% of worms only fed *pgl-1* RNAi, and in 30% only fed *glh-1* RNAi. We also observed an expanded *msp-3* domain in 18% of *glh-4(gk224) glh-1(ok439)* double mutants, in 31% of *pgl-1(bn101)* single mutants and in 20% of *pgl-3(bn104)* single mutants. Proximal germlines in *pgl-1(bn101); pgl-3(bn104)* did not show an expansion of the *msp-3* domain, but these double mutants contained very severe germline proliferation defects that might have masked this phenotype. Our results suggest that the distal expansion of sperm-specific mRNAs can be caused by compromising P-granule integrity in several genetic backgrounds. The percentage of *csr-1* animals showing *msp-3* expansion did not increase in a *pgl-1(bn101)* background, possibly due to *pgl-1* mutants being partially RNAi defective (Robert et al., 2005), but increased to 65% in *pgl-3(bn104)* mutants (supplementary material Fig. S6; Table 1). One interpretation is that the effects of CSR-1 and PGL-3 on *msp-3* expansion are additive, and that *csr-1* RNAi further compromises P granules to suppress the accumulation or transcription of sperm-specific mRNAs. A second interpretation is that *csr-1* is epistatic to P granules, and that partial CSR-1 activity remains when P granules are disrupted. Because *csr-1* mutants are RNAi defective with severe germline defects, attempts to distinguish these two interpretations were inconclusive.

P granules and CSR-1 repress spermatogenesis through the germline sex determination pathway

Sperm-specific mRNA expression is regulated by the germline sex-determination pathway [reviewed by Zanetti and Puoti (2013)]. This pathway converges to increase the expression of FOG-3 during the L3-L4 stages of development in the *C. elegans* hermaphrodite. Expression of FOG-3 initiates sperm fate specification through unknown mechanisms. Almost half of the genes known to act upstream of FOG-3 in the germline sex determination pathway co-localize with P granules (Ariz et al., 2009; Draper et al., 1996; Eckmann et al., 2002; Jones et al., 1996; Rybarska et al., 2009; Voronina et al., 2012), and include proteins that promote (GLD-1 and GLD-3) and repress (MEX-3, PUF-8, GLS-1 and FBF-2) FOG-3 expression. We found that *fog-3* transcription is upregulated following P-granule RNAi (1.5-fold) and *csr-1* RNAi (9.5-fold, supplementary material Table S1), suggesting that the increase in sperm-specific transcription is dependent upon FOG-3. Other P-granule components known to promote proper spermatogenesis include the mRNA cap-binding protein IFE-1 (Amiri et al., 2001; Henderson et al., 2009), and the Argonautes ALG-3 and ALG-4 (Conine et al., 2010, 2013). To determine whether the expansion of *msp-3* transcripts is dependent upon these P-granule components, P-granule, *pgl-1;pgl-3* and *csr-1* RNAi was performed in *ife-1(bn127)* mutants, *alg-4(ok1041); alg-3 (tm1155)* double mutants, and *fog-3(q470)* loss-of-function heterozygous mutants (supplementary material Fig. S6; Table 1). *ife-1(bn127)* single mutants and *alg-4(ok1041); alg-3(tm1155)* double mutants did not suppress *msp-3* expansion upon *csr-1*, P-granule and *pgl-1; pgl-3* depletion. Similarly, *msp-3* expansion was not suppressed in *fog-3(q470/+)* heterozygotes. However, *msp-3* transcripts are absent in *fog-3(q470)* homozygotes. This shows that CSR-1 and P granules either act indirectly to limit the extent to which *fog-3* is expressed, or that spermatogenesis must first initiate in order to observe the distal expansion of sperm-gene expression. The large increase in *fog-3* expression that is observed after *csr-1* RNAi supports the former possibility, but cannot exclude the latter.

To determine how *fog-3* is regulated, P-granule and *csr-1* germline mRNA-seq data were examined for expression changes in genes known to act upstream in the germline sex determination pathway. We found that transcription of *her-1* is increased 1.8- and 6.6-fold following P-granule and *csr-1* RNAi, respectively. Hermaphrodites do not normally express *her-1* mRNA. Instead, during the short window of spermatogenesis, hermaphrodites promote FOG-3 activity through other germline sex determination components. Therefore, one possibility is that P granules and CSR-1 negatively regulate *fog-3* expression by suppressing *her-1* transcript accumulation in the hermaphrodite germline.

DISCUSSION

We initially set out to test whether P granules maintain germline pluripotency by antagonizing the transcription or accumulation of somatic mRNAs. Instead, we discovered that most transcripts previously thought to be soma specific might already be expressed at low levels in the germline, suggesting that P granules inhibit translation and not the accumulation of these somatic mRNAs, and follow-up studies will need to determine whether this is the case. We also found that P granules and CSR-1 suppress the accumulation of sperm-specific transcripts in the germline of adult hermaphrodites. This does not come as a complete surprise, as the role of both germ granules and endogenous siRNA pathways in spermatogenesis is well documented in a number of species [reviewed by Yadav and Kotaja (2014)]. In *C. elegans*, the RNA-directed RNA polymerase EGO-1 functions to produce the 22G siRNAs bound by CSR-1, and *ego-1* mutants prolong spermatogenesis and produce small 'intersexual' gametes before making recognizable oocytes (Smardon et al., 2000). Because these intersexual gametes are not produced in *ego-1 fog-3* germlines, it was proposed that EGO-1 in some

Development (2015) 142, 1745-1755 doi:10.1242/dev.121434

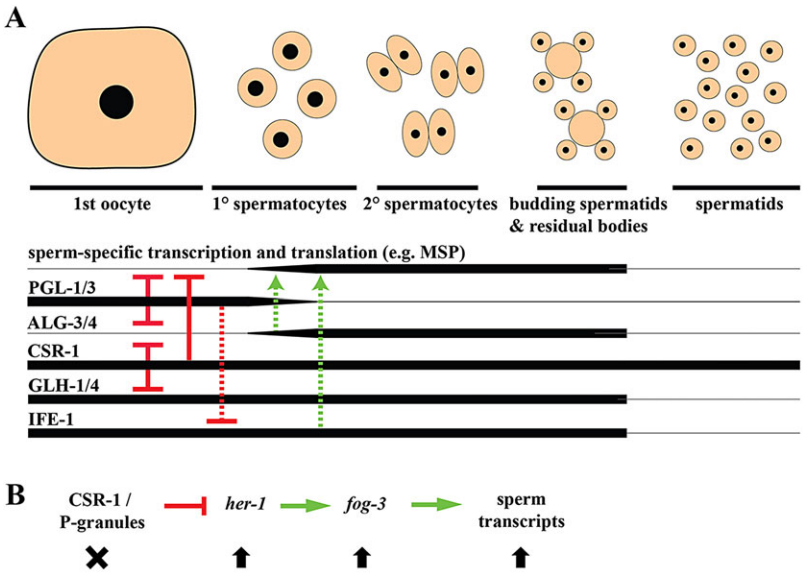

Fig. 5. Model for P-granule and CSR-1 function in the hermaphrodite germline. (A) In germ cells, CSR-1 and PGL-1/3 repress *alg-3/4* and sperm-specific transcription. As PGL-1/3 begins to disassemble in primary spermatocytes, factors like ALG-3/4 and IFE-1 promote the transcription and translation of sperm-specific mRNAs. When spermatogenesis completes in *C. elegans* hermaphrodites, P-granule and CSR-1 expression promotes oocyte development and maturation. Dotted lines as previously proposed in Amiri et al. (2001); Conine et al. (2013). (B) P granules and CSR-1 repress *her-1*, *fog-3* and sperm-specific transcription. When P-granule or CSR-1 function is impaired, *her-1* transcription is increased, promoting *fog-3* expression and sperm transcription.

way promotes the sperm-oocyte switch. Sperm genes are also overexpressed in *eri-1* and *rrf-3* mutants (Asikainen et al., 2007), both of which encode Dicer complex components that produce 26G endo-siRNAs complementing spermatogenesis genes (Gent et al., 2009; Han et al., 2009; Pavelec et al., 2009). It has been proposed that spermatogenesis defects observed when impairing ERI-1, RRF-3 or the sperm-specific 26G-binding proteins ALG-3 and ALG-4 can be attributed to either under- or overexpression of sperm mRNAs (Conine et al., 2010; Gent et al., 2009; Han et al., 2009; Pavelec et al., 2009). This apparent discrepancy might have a simple resolution if an endogenous siRNA pathway represses sperm-specific transcription in adult hermaphrodites that have already undergone spermatogenesis, but promotes sperm-specific transcription in males and during the short window of spermatogenesis in hermaphrodites.

Our model is that both P granules and CSR-1 function to regulate the switch between sperm-specific activation and repression. Spermatogenesis occurs during the L4 stage of hermaphrodite development, but sperm transcription must be suppressed in the first wave of germ cells that develop into oocytes (Fig. 5A). A clear boundary must then be maintained between male and female germ cells until spermatogenesis is complete. Defects observed in proximal germ cells following *csr-1* or P-granule RNAi were suppressed by inhibiting spermatogenesis, suggesting that germ cell crowding and premature cellularization in these worms are the result of partial masculinization. Our data suggest that P-granule components such as PGL-1 and PGL-3 act to define the boundary between spermatogenesis and oogenesis, and function with CSR-1 to suppress sperm-specific transcription. CSR-1 function might require perinuclear localization to interact with nascent mRNAs exiting P granules, and, in turn, P-granule integrity might depend on the ability of CSR-1 to escort highly expressed target mRNAs through and away from P granules. One model is that CSR-1-bound 22G RNAs simply correspond to germline transcripts that are most abundantly expressed. In complying with this model, when spermatogenesis is initiated and ALG-3 and ALG-4 are expressed, 26G RNAs that correspond to sperm genes are processed into CSR-1-bound 22G RNAs, which are then used to chaperone newly abundant sperm transcripts through P granules. In adult hermaphrodite germlines, the accumulation of CSR-1-targeted mRNAs does not change following *csr-1* RNAi, supporting a more passive model in which CSR-1 primarily functions to chaperone its target mRNAs instead of regulating their accumulation.

If this passive model for CSR-1 and its bound 22Gs is correct, how do P granules and CSR-1 first promote the switch from spermatogenesis to oogenesis in the hermaphrodite? Our results suggest that they do so by regulating the germline sex determination pathway (Fig. 5B). Transcripts encoding FOG-3 were significantly upregulated when CSR-1 or P granules were impaired, and feminized *fog-3* and *fem-3* loss-of-function animals fully suppressed sperm-specific transcription. Similar results were observed previously with the loss of *eri-1*. Whereas *eri-1* mutants exhibit increased sperm transcription in the germline, this is suppressed in *fem-3* worms (Pavelec et al., 2009). Whereas our results suggest that CSR-1 and P granules repress *her-1* in the germline, there are additional possibilities that could explain how CSR-1 and P granules regulate the germline sex determination pathway. For example, IFET-1 is an eIF4E-transporter in *C. elegans* that recruits a number of translational repressors to P granules, and impairing its function is sufficient to promote masculinization in the hermaphrodite germline (Sengupta et al., 2013). IFET-1 activity might require intact P granules. Another study shows that the germline sex determination pathway component, FBF-2, requires PGL-1 and P-granule recruitment to bind to and silence the translation of its mRNA targets in the more distal germline (Voronina et al., 2012). Both *fem-3* and *fog-3* are known FBF-2 targets [reviewed by Zanetti and Puoti (2013)]. A final study shows that the germline sex determination component FBF-1 forms a complex with EFT-3/eEF1A and CSR-1 in *C. elegans* lysates (Friend et al., 2012). This study also shows that CSR-1 represses the accumulation FBF targets *gld-1* and *cye-1*, whereas the CSR-1 cofactors DRH-3, EGO-1 and EKL-1 do not. Therefore, the role of CSR-1 in regulating the germline sex determination pathway might be independent from the sequence of bound 22G siRNAs, instead acting through a conserved PUF-Ago-eEF1A complex that attenuates translational elongation of its mRNA targets. Although it is clear that P granules and CSR-1 regulate the germline sex determination pathway, the specifics of this regulation still need to be resolved.

MATERIALS AND METHODS

Strain maintenance

C. elegans strains were maintained as per standard protocols (Brenner, 1974). The following strains were used and can be obtained through the CGC: N2(Bristol), SS579 *pgl-1(bn101)* IV, SS608 *pgl-3(bn104)* V, KB4 *glh-4(gk255) glh-1(ok439)* I/*hT2[bli-4(e937) let-?(q782) qIs48]* I;III,

Development (2015) 142, 1745-1755 doi:10.1242/dev.121434

SS615 *pgl-1(bn101) unc-24(e138)* IV; *pgl-3(bn104) dpy-11(e224)* V, SS712 *ife-1(bn127)* III, WM300 *alg-4(ok1041)* III; *alg-3(tm1155)* IV, JK1403 *fog-3(q470)/unc-13(e1091) lin-11(n566)* I, CB3844 *fem-3(e2006)* IV and TH206 *[pgl-1p::PGL-1::TY1::EGFP::3xFLAG(92C12)::pgl-1 3′ UTR + Cbr-unc-119(+)]* I. DG3913 *lin-41(tn1541[GFP::tev::s::LIN-41])* I was kindly provided by David Greenstein (Spike et al., 2014).

RNAi

P-granule RNAi (simultaneously targeting *pgl-1, pgl-3, glh-1* and *glh-4*) has been described previously (Updike et al., 2014). The *pgl-1;pgl-3* RNAi construct (pDU51) contains 320- and 349-base pair fragments from *pgl-1*(1374-1666) and *pgl-3*(265-613), respectively, cloned into L4440 and transformed into HT115 bacteria. *csr-1* and *pgl-1* RNAi was obtained from the Ahringer Library (Kamath et al., 2003). The *glh-1* RNAi construct was described in Spike et al. (2008b). Control RNAi contained the L4440 plasmid in HT115 bacteria. RNAi was performed at 24°C for mRNA-seq experiments. RNAi feeding for FISH experiments was started on L1 P0 animals at 20°C; their F1 larval progeny were raised at 24°C and maintained through the F2 generation before being imaged as young F2 adults. CB3844 animals were fed RNAi at 15°C (P0, F1 generations) and their F2 larval progeny were shifted to 24°C.

Germline dissections

RNAi feeding (empty vector, P-granule or *csr-1*) was started in L1 staged worms at 24°C; and germlines were dissected from their F1 progeny. Anti-PGL-1 antibody staining was performed in parallel to verify RNAi knockdown. Total RNA was collected from young adult hermaphrodite germlines (those with a vulva, one day past the L4 stage). Mouth-pipetting with a pulled capillary needle was used to isolate the gonad at the dorsal-to-ventral bend (supplementary material Fig. S1). Germlines were dissected in egg buffer (25 mM HEPES, 120 mM NaCl, 2 mM $MgCl_2$, 2 mM $CaCl_2$, 50 mM KCl, 0.5% Tween-20 and 1 mM levamisole) and immediately dispensed into Trizol (Life Technologies) on ice, and a total of 400-500 dissected germlines were collected for each replicate. RNA isolation proceeded as previously described (Gaydos et al., 2012), resulting in total RNA ranging from 1.5 to 4 µg per replicate sample, which was sufficient to sequence without linear amplification.

mRNA-sequencing and analysis

Four biological replicates of each condition (empty vector control, P-granule RNAi and CSR-1 RNAi germlines) were collected for total RNA. Using a TruSeq RNAv2 kit (Illumina), mRNA was polyA-selected, fragmented and used to create adapter-ligated cDNA for sequencing. One hundred base pair sequences were obtained on an Illumina HiSeq2500 and processed as single-end reads using the following pipeline: TopHat2 (v.2.0.8b) was run as described in Kim et al. (2013), using the WBcel215 assembly and a provided transcript annotation file (Ensembl release 70) retrieved from Illumina iGenomes (http://support.illumina.com/sequencing/sequencing_software/igenome.html) (Kersey et al., 2014). HTSeq (v.0.5.4p3) was then used to generate read counts per gene per sample and those counts were normalized across samples with DESeq (v.1.1.2.1) (Anders and Huber, 2010; Anders et al., 2015). Default parameters were used in most instances, with the following exceptions: *-G, -M* arguments were used in the TopHat2 protocol; *-m union* was specified in the *htseq-count* command; *method="blind"* was used for dispersion estimation in DESeq. Fold change between the average of the four control replicates and the average of the four test replicates was used to calculate the significance using a negative binomial distribution. An adjusted *P*-value was calculated using the Benjamini–Hochberg method for multiple testing correction (Anders and Huber, 2010). Gene ontology was evaluated via Gorilla (Eden et al., 2009). The UCSC Genome Browser (Kent et al., 2002) was used to visualize aligned reads. P-granule RNAi dataset: Set 1 transcripts were defined as those with a *P*-value <0.05 and an expression change of at least >twofold over control. Set 2 transcripts had an adjusted *P*-value <0.05 and an expression change >3.6-fold over control. csr-1 RNAi dataset: Set 1 transcripts were defined as those with a *P*-value <0.05 and an expression change of >1.9-fold over control. Set 2 transcripts were defined as those with an adjusted *P*-value <0.05 and an expression change of >2.6-fold over control. mRNA-seq data have been deposited at the GEO database under the accession number GSE67954.

Antibody staining

SP56 (Ward et al., 1986) staining was performed on dissected germlines as previously described (Updike et al., 2014).

Fluorescent *in situ* hybridization (FISH)

Stellaris FISH probes (Biosearch Technologies) were designed for *msp-3*, *ssq-1*, *rmd-3*, *unc-16* and *hbl-1* with CAL Fluor Red 610. Whole-worm FISH for *msp-3*, *ssq-1* and *rmd-3* was performed as described by Ji and van Oudenaarden (2012) with the following modifications: worms were incubated in fix for 30 min, not 45, and kept rotating in ethanol at 4°C for 48 h, not 24. After the ethanol incubation, worms were resuspended in 1 ml wash buffer for 8 min. Worms were hybridized using ∼2.5 µl probe (at 25 µM stock oligo concentration) per worm plate washed, and incubated at 37°C for 4 h. The animals were dropped on GCP (0.2% w/v gelatin, 0.02% w/v chrome alum, 0.05% w/v poly-L-lysine)-coated slides, placed under a coverslip with 2× SSC and imaged. *unc-16* and *hbl-1* FISH was performed on dissected germlines as previously described (Updike et al., 2014). Images were acquired and deconvolved using Leica AF6000 acquisition software on an inverted microscope (Leica DMI6000B) with a cooled CCD camera (Leica DFC365FX) and a Leica 40× air objective with a 0.5 µm *z*-stack. Expanded *msp-3*, *ssq-1* and *rmd-3* expression was identified as expression expanding distally from the proximal germline past the bend region of the gonad.

Acknowledgements

We would like to thank Ben King at the MDI Biological Laboratory Comparative Functional Genomics Core for assistance with data analysis, the Genome Technologies division at the Jackson Laboratory which performed the mRNA-seq experiments, David Greenstein and Caroline Spike (University of Minnesota, MN, USA), and Susan Strome (University of California Santa Cruz, CA, USA) for reagents and discussions, and the *C. elegans* Genetics Center NIH-ORIP [P40 OD010440] for strains.

Competing interests

The authors declare no competing or financial interests.

Author contributions

A.C.C. performed RNAi, mRNA-seq mapping and differential expression analysis, FISH and imaging. A.C.C. and D.L.U. performed the germline dissections and mRNA-seq experiments, mRNA-seq analysis, and collaborated on the experimental design and manuscript.

Funding

A.C.C. and D.L.U. used equipment obtained through an Institutional Development Award (IDeA) from the National Institutes of Health-National Institute of General Medical Sciences (NIH-NIGMS) [P20GM103423]. A.C.C. and D.L.U.'s work, as well as B.K. at the Comparative Functional Genomics Core, is supported by an IDeA Center of Biomedical Research Excellence award from the NIH-NIGMS [P20GM104318]. The work of A.C.C. and D.L.U. work is also supported by NIH-NIGMS [R01GM113933]. Deposited in PMC for release after 12 months.

Supplementary material

Supplementary material available online at
http://dev.biologists.org/lookup/suppl/doi:10.1242/dev.121434/-/DC1

References

Amiri, A., Keiper, B. D., Kawasaki, I., Fan, Y., Kohara, Y., Rhoads, R. E. and Strome, S. (2001). An isoform of eIF4E is a component of germ granules and is required for spermatogenesis in C. elegans. *Development* **128**, 3899-3912.

Anders, S. and Huber, W. (2010). Differential expression analysis for sequence count data. *Genome Biol.* **11**, R106.

Anders, S., Pyl, P. T. and Huber, W. (2015). HTSeq A Python framework to work with high-throughput sequencing data. *Bioinformatics* **31**, 166-169.

Ariz, M., Mainpal, R. and Subramaniam, K. (2009). C. elegans RNA-binding proteins PUF-8 and MEX-3 function redundantly to promote germline stem cell mitosis. *Dev. Biol.* **326**, 295-304.

Asikainen, S., Storvik, M., Lakso, M. and Wong, G. (2007). Whole genome microarray analysis of C. elegans rrf-3 and eri-1 mutants. *FEBS Lett.* **581**, 5050-5054.

Avgousti, D. C., Palani, S., Sherman, Y. and Grishok, A. (2012). CSR-1 RNAi pathway positively regulates histone expression in C. elegans. *EMBO J.* **31**, 3821-3832.
Brenner, S. (1974). The genetics of Caenorhabditis elegans. *Genetics* **77**, 71-94.
Cecere, G., Hoersch, S., O'Keeffe, S., Sachidanandam, R. and Grishok, A. (2014). Global effects of the CSR-1 RNA interference pathway on the transcriptional landscape. *Nat. Struct. Mol. Biol.* **21**, 358-365.
Chu, D. S. and Shakes, D. C. (2013). Spermatogenesis. *Adv. Exp. Med. Biol.* **757**, 171-203.
Chu, D. S., Liu, H., Nix, P., Wu, T. F., Ralston, E. J., Yates, J. R., III and Meyer, B. J. (2006). Sperm chromatin proteomics identifies evolutionarily conserved fertility factors. *Nature* **443**, 101-105.
Claycomb, J. M., Batista, P. J., Pang, K. M., Gu, W., Vasale, J. J., van Wolfswinkel, J. C., Chaves, D. A., Shirayama, M., Mitani, S., Ketting, R. F. et al. (2009). The Argonaute CSR-1 and its 22G-RNA cofactors are required for holocentric chromosome segregation. *Cell* **139**, 123-134.
Conine, C. C., Batista, P. J., Gu, W., Claycomb, J. M., Chaves, D. A., Shirayama, M. and Mello, C. C. (2010). Argonautes ALG-3 and ALG-4 are required for spermatogenesis-specific 26G-RNAs and thermotolerant sperm in Caenorhabditis elegans. *Proc. Natl. Acad. Sci. USA* **107**, 3588-3593.
Conine, C. C., Moresco, J. J., Gu, W., Shirayama, M., Conte, D., Yates, J. R. and Mello, C. C. (2013). Argonautes promote male fertility and provide a paternal memory of germline gene expression in C. elegans. *Cell* **155**, 1532-1544.
Draper, B. W., Mello, C. C., Bowerman, B., Hardin, J. and Priess, J. R. (1996). MEX-3 is a KH domain protein that regulates blastomere identity in early C. elegans embryos. *Cell* **87**, 205-216.
Eckmann, C. R., Kraemer, B., Wickens, M. and Kimble, J. (2002). GLD-3, a bicaudal-C homolog that inhibits FBF to control germline sex determination in C. elegans. *Dev. Cell* **3**, 697-710.
Eden, E., Navon, R., Steinfeld, I., Lipson, D. and Yakhini, Z. (2009). GOrilla: a tool for discovery and visualization of enriched GO terms in ranked gene lists. *BMC Bioinformatics* **10**, 48.
Friend, K., Campbell, Z. T., Cooke, A., Kroll-Conner, P., Wickens, M. P. and Kimble, J. (2012). A conserved PUF-Ago-eEF1A complex attenuates translation elongation. *Nat. Struct. Mol. Biol.* **19**, 176-183.
Gaydos, L. J., Rechtsteiner, A., Egelhofer, T. A., Carroll, C. R. and Strome, S. (2012). Antagonism between MES-4 and Polycomb repressive complex 2 promotes appropriate gene expression in C. elegans germ cells. *Cell Rep.* **2**, 1169-1177.
Gent, J. I., Schvarzstein, M., Villeneuve, A. M., Gu, S. G., Jantsch, V., Fire, A. Z. and Baudrimont, A. (2009). A Caenorhabditis elegans RNA-directed RNA polymerase in sperm development and endogenous RNA interference. *Genetics* **183**, 1297-1314.
Gruidl, M. E., Smith, P. A., Kuznicki, K. A., McCrone, J. S., Kirchner, J., Roussell, D. L., Strome, S. and Bennett, K. L. (1996). Multiple potential germ-line helicases are components of the germ-line-specific P granules of Caenorhabditis elegans. *Proc. Natl. Acad. Sci. USA* **93**, 13837-13842.
Gu, W., Shirayama, M., Conte, D., Vasale, J., Batista, P. J., Claycomb, J. M., Moresco, J. J., Youngman, E. M., Keys, J., Stoltz, M. J. et al. (2009). Distinct argonaute-mediated 22G-RNA pathways direct genome surveillance in the C. elegans germline. *Mol. Cell* **36**, 231-244.
Han, T., Manoharan, A. P., Harkins, T. T., Bouffard, P., Fitzpatrick, C., Chu, D. S., Thierry-Mieg, D., Thierry-Mieg, J. and Kim, J. K. (2009). 26G endo-siRNAs regulate spermatogenic and zygotic gene expression in Caenorhabditis elegans. *Proc. Natl. Acad. Sci. USA* **106**, 18674-18679.
Henderson, M. A., Cronland, E., Dunkelbarger, S., Contreras, V., Strome, S. and Keiper, B. D. (2009). A germline-specific isoform of eIF4E (IFE-1) is required for efficient translation of stored mRNAs and maturation of both oocytes and sperm. *J. Cell Sci.* **122**, 1529-1539.
Illmensee, K. and Mahowald, A. P. (1974). Transplantation of posterior polar plasm in Drosophila. Induction of germ cells at the anterior pole of the egg. *Proc. Natl. Acad. Sci. USA* **71**, 1016-1020.
Ji, N. and van Oudenaarden, A. (2012). Single molecule fluorescent in situ hybridization (smFISH) of C. elegans worms and embryos. *WormBook* **13**, 1-16.
Jones, A. R., Francis, R. and Schedl, T. (1996). GLD-1, a cytoplasmic protein essential for oocyte differentiation, shows stage- and sex-specific expression during Caenorhabditis elegans germline development. *Dev. Biol.* **180**, 165-183.
Kamath, R. S., Fraser, A. G., Dong, Y., Poulin, G., Durbin, R., Gotta, M., Kanapin, A., Le Bot, N., Moreno, S., Sohrmann, M. et al. (2003). Systematic functional analysis of the Caenorhabditis elegans genome using RNAi. *Nature* **421**, 231-237.
Kasper, D. M., Gardner, K. E. and Reinke, V. (2013). Homeland security in the C. elegans germ line: insights into the biogenesis and function of piRNAs. *Epigenetics* **9**, 1-13.
Kawasaki, I., Shim, Y.-H., Kirchner, J., Kaminker, J., Wood, W. B. and Strome, S. (1998). PGL-1, a predicted RNA-binding component of germ granules, is essential for fertility in C. elegans. *Cell* **94**, 635-645.
Kawasaki, I., Amiri, A., Fan, Y., Meyer, N., Dunkelbarger, S., Motohashi, T., Karashima, T., Bossinger, O. and Strome, S. (2004). The PGL family proteins associate with germ granules and function redundantly in Caenorhabditis elegans germline development. *Genetics* **167**, 645-661.
Kawasaki, I., Jeong, M.-H. and Shim, Y.-H. (2011). Regulation of sperm-specific proteins by IFE-1, a germline-specific homolog of eIF4E, in C. elegans. *Mol. Cells* **31**, 191-197.
Kent, W. J., Sugnet, C. W., Furey, T. S., Roskin, K. M., Pringle, T. H., Zahler, A. M. and Haussler, D. (2002). The human genome browser at UCSC. *Genome Res.* **12**, 996-1006.
Kersey, P. J., Allen, J. E., Christensen, M., Davis, P., Falin, L. J., Grabmueller, C., Hughes, D. S. T., Humphrey, J., Kerhornou, A., Khobova, J. et al. (2014). Ensembl Genomes 2013: scaling up access to genome-wide data. *Nucleic Acids Res.* **42**, D546-D552.
Kim, D., Pertea, G., Trapnell, C., Pimentel, H., Kelley, R. and Salzberg, S. L. (2013). TopHat2: accurate alignment of transcriptomes in the presence of insertions, deletions and gene fusions. *Genome Biol.* **14**, R36.
Kulkarni, M., Shakes, D. C., Guevel, K. and Smith, H. E. (2012). SPE-44 implements sperm cell fate. *PLoS Genet.* **8**, e1002678.
Lee, H.-C., Gu, W., Shirayama, M., Youngman, E., Conte, D. and Mello, C. C. (2012). C. elegans piRNAs mediate the genome-wide surveillance of germline transcripts. *Cell* **150**, 78-87.
Merritt, C., Rasoloson, D., Ko, D. and Seydoux, G. (2008). 3′ UTRs are the primary regulators of gene expression in the C. elegans germline. *Curr. Biol.* **18**, 1476-1482.
Ortiz, M. A., Noble, D., Sorokin, E. P. and Kimble, J. (2014). A New Dataset of Spermatogenic vs. Oogenic Transcriptomes in the Nematode Caenorhabditis elegans. *G3* **4**, 1765-1772.
Pavelec, D. M., Lachowiec, J., Duchaine, T. F., Smith, H. E. and Kennedy, S. (2009). Requirement for the ERI/DICER complex in endogenous RNA interference and sperm development in Caenorhabditis elegans. *Genetics* **183**, 1283-1295.
Rechtsteiner, A., Ercan, S., Takasaki, T., Phippen, T. M., Egelhofer, T. A., Wang, W., Kimura, H., Lieb, J. D. and Strome, S. (2010). The histone H3K36 methyltransferase MES-4 acts epigenetically to transmit the memory of germline gene expression to progeny. *PLoS Genet.* **6**, e1001091.
Reinke, V., Gil, I. S., Ward, S. and Kazmer, K. (2004). Genome-wide germline-enriched and sex-biased expression profiles in Caenorhabditis elegans. *Development* **131**, 311-323.
Robert, V. J. P., Sijen, T., van Wolfswinkel, J. and Plasterk, R. H. A. (2005). Chromatin and RNAi factors protect the C. elegans germline against repetitive sequences. *Genes Dev.* **19**, 782-787.
Rybarska, A., Harterink, M., Jedamzik, B., Kupinski, A. P., Schmid, M. and Eckmann, C. R. (2009). GLS-1, a novel P-granule component, modulates a network of conserved RNA regulators to influence germ cell fate decisions. *PLoS Genet.* **5**, e1000494.
Sengupta, M. S. and Boag, P. R. (2012). Germ granules and the control of mRNA translation. *IUBMB Life* **64**, 586-594.
Sengupta, M. S., Low, W. Y., Patterson, J. R., Kim, H.-M., Traven, A., Beilharz, T. H., Colaiácovo, M. P., Schisa, J. A. and Boag, P. R. (2013). ifet-1 is a broad-scale translational repressor required for normal P-granule formation in C. elegans. *J. Cell Sci.* **126**, 850-859.
Seth, M., Shirayama, M., Gu, W., Ishidate, T., Conte, D. and Mello, C. C. (2013). The C. elegans CSR-1 argonaute pathway counteracts epigenetic silencing to promote germline gene expression. *Dev. Cell* **27**, 656-663.
Sheth, U., Pitt, J., Dennis, S. and Priess, J. R. (2010). Perinuclear P granules are the principal sites of mRNA export in adult C. elegans germ cells. *Development* **137**, 1305-1314.
Shim, Y. H. (1999). elt-1, a gene encoding a Caenorhabditis elegans GATA transcription factor, is highly expressed in the germ lines with msp genes as the potential targets. *Mol. Cells* **9**, 535-541.
Shirayama, M., Seth, M., Lee, H.-C., Gu, W., Ishidate, T., Conte, D.Jr and Mello, C. C. (2012). piRNAs initiate an epigenetic memory of nonself RNA in the C. elegans germline. *Cell* **150**, 65-77.
Smardon, A., Spoerke, J. M., Stacey, S. C., Klein, M. E., Mackin, N. and Maine, E. M. (2000). EGO-1 is related to RNA-directed RNA polymerase and functions in germ-line development and RNA interference in C. elegans. *Curr. Biol.* **10**, 169-178.
Spike, C. A., Bader, J., Reinke, V. and Strome, S. (2008a). DEPS-1 promotes P-granule assembly and RNA interference in C. elegans germ cells. *Development* **135**, 983-993.
Spike, C., Meyer, N., Racen, E., Orsborn, A., Kirchner, J., Kuznicki, K., Yee, C., Bennett, K. and Strome, S. (2008b). Genetic analysis of the Caenorhabditis elegans GLH family of P-granule proteins. *Genetics* **178**, 1973-1987.
Spike, C. A., Coetzee, D., Eichten, C., Wang, X., Hansen, D. and Greenstein, D. I. (2014). The TRIM-NHL protein LIN-41 and the OMA RNA-binding proteins antagonistically control the prophase-to-metaphase transition and growth of Caenorhabditis elegans oocytes. *Genetics* **198**, 1535-1558.
Strome, S. and Wood, W. B. (1982). Immunofluorescence visualization of germ-line-specific cytoplasmic granules in embryos, larvae, and adults of Caenorhabditis elegans. *Proc. Natl. Acad. Sci. USA* **79**, 1558-1562.

Development (2015) 142, 1745-1755 doi:10.1242/dev.121434

Tada, H., Mochii, M., Orii, H. and Watanabe, K. (2012). Ectopic formation of primordial germ cells by transplantation of the germ plasm: direct evidence for germ cell determinant in Xenopus. *Dev. Biol.* **371**, 86-93.

Updike, D. L. and Strome, S. (2009). A genomewide RNAi screen for genes that affect the stability, distribution and function of P granules in Caenorhabditis elegans. *Genetics* **183**, 1397-1419.

Updike, D. and Strome, S. (2010). P-granule assembly and function in Caenorhabditis elegans germ cells. *J. Androl.* **31**, 53-60.

Updike, D. L., Hachey, S. J., Kreher, J. and Strome, S. (2011). P-granules extend the nuclear pore complex environment in the C. elegans germ line. *J. Cell Biol.* **192**, 939-948.

Updike, D. L., Knutson, A. K., Egelhofer, T. A., Campbell, A. C. and Strome, S. (2014). Germ-granule components prevent somatic development in the C. elegans germline. *Curr. Biol.* **24**, 970-975.

Voronina, E., Paix, A. and Seydoux, G. (2012). The P-granule component PGL-1 promotes the localization and silencing activity of the PUF protein FBF-2 in germline stem cells. *Development* **139**, 3732-3740.

Vought, V. E., Ohmachi, M., Lee, M.-H. and Maine, E. M. (2005). EGO-1, a putative RNA-directed RNA polymerase, promotes germline proliferation in parallel with GLP-1/notch signaling and regulates the spatial organization of nuclear pore complexes and germline P granules in Caenorhabditis elegans. *Genetics* **170**, 1121-1132.

Ward, S., Roberts, T. M., Strome, S., Pavalko, F. M. and Hogan, E. (1986). Monoclonal antibodies that recognize a polypeptide antigenic determinant shared by multiple Caenorhabditis elegans sperm-specific proteins. *J. Cell Biol.* **102**, 1778-1786.

Watson, J. D., Wang, S., Von Stetina, S. E., Spencer, W. C., Levy, S., Dexheimer, P. J., Kurn, N., Heath, J. D. and Miller, D. M. (2008). Complementary RNA amplification methods enhance microarray identification of transcripts expressed in the C. elegans nervous system. *BMC Genomics* **9**, 84.

Wedeles, C. J., Wu, M. Z. and Claycomb, J. M. (2013). Protection of germline gene expression by the C. elegans argonaute CSR-1. *Dev. Cell* **27**, 664-671.

Wedeles, C. J., Wu, M. Z. and Claycomb, J. M. (2014). Silent no more: endogenous small RNA pathways promote gene expression. *Worm* **3**, e28641.

Yadav, R. P. and Kotaja, N. (2014). Small RNAs in spermatogenesis. *Mol. Cell. Endocrinol.* **382**, 498-508.

Zanetti, S. and Puoti, A. (2013). Sex determination in the Caenorhabditis elegans germline. *Adv. Exp. Med. Biol.* **757**, 41-69.

SUPPLEMENTARY FIGURES

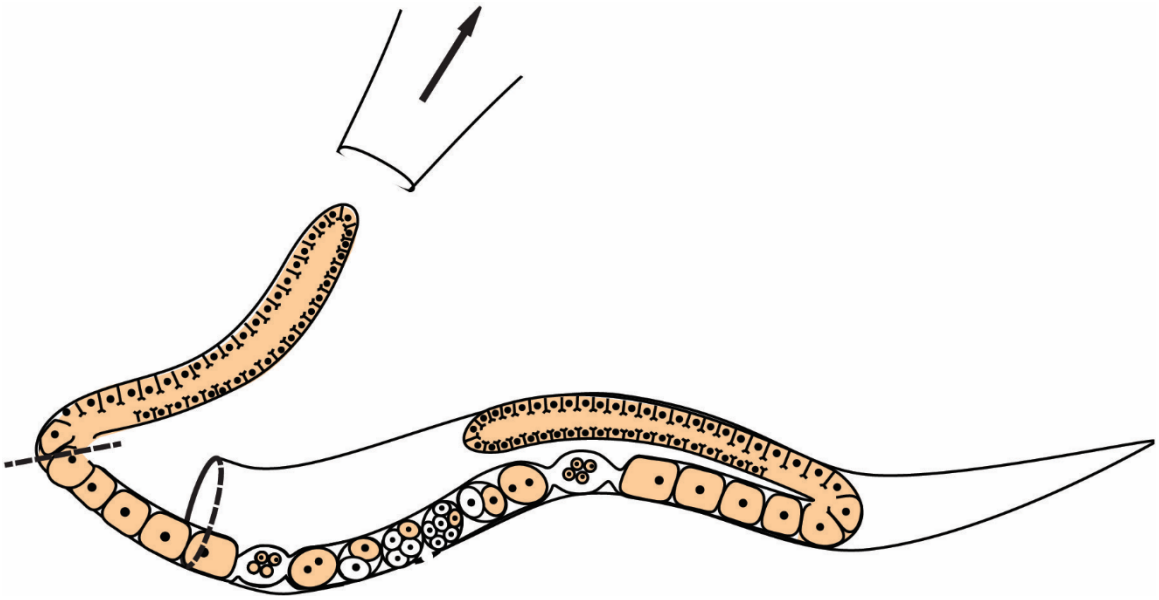

Figure S1. Germline dissection method. Heads were removed with 27.5 gauge needles, allowing the distal portion of the germline to pop out of the worm. Glass capillaries pulled with an opening just large enough to fit the end of the germline were used to rapidly detach them at the ventral to distal bend, eliminating the need to first dissect germlines away from the worm, while at the same time excluding more mature oocytes and the spermatheca from samples. Detached germlines were suctioned using an aspirator tube assembly system (Sigma A5177). Using this method instead of first detaching germlines with a scalpel improved sample consistency and allowed us to harvest approximately five times as many germlines in the same duration.

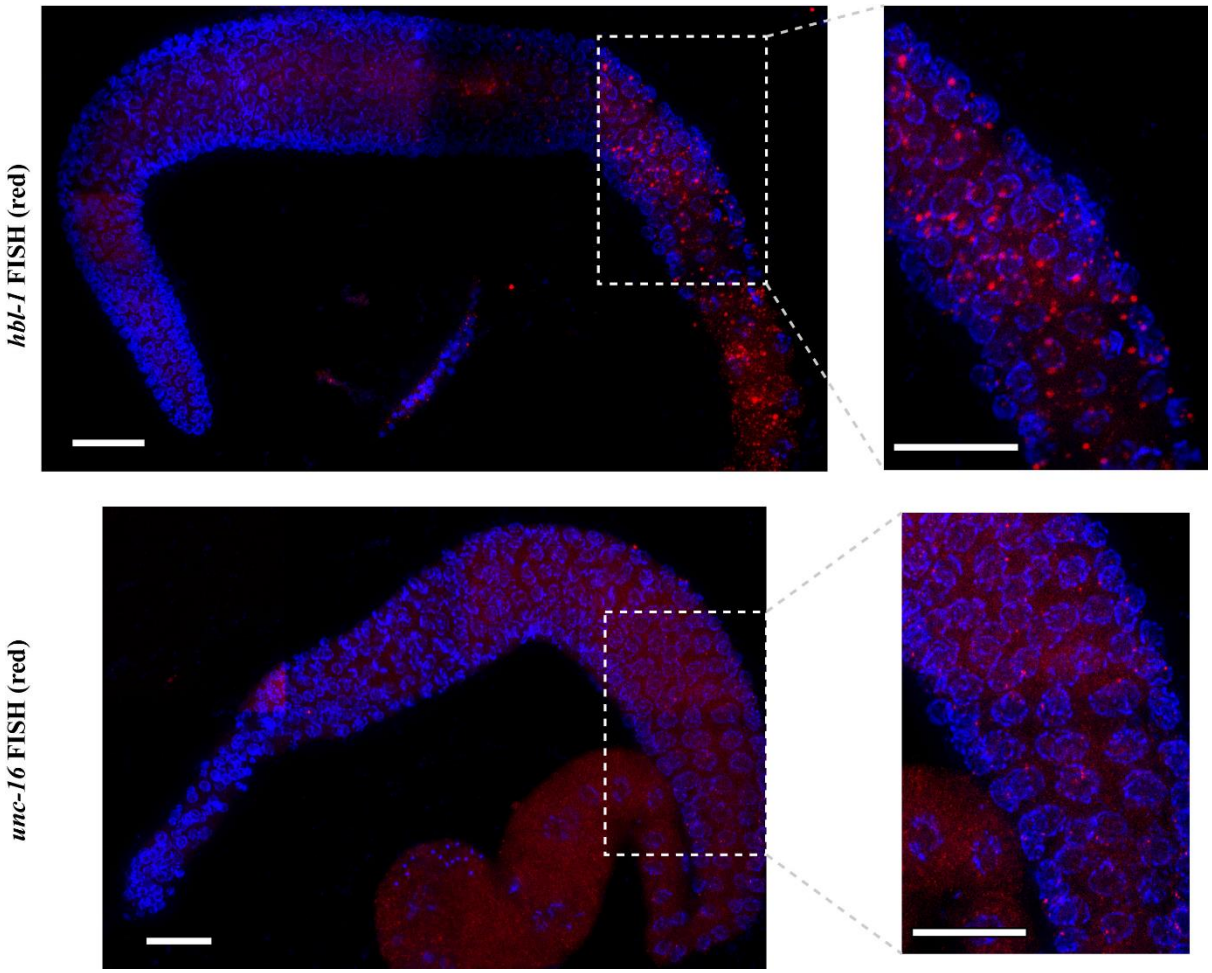

Figure S2. Germline expression of soma-specific transcripts. *hbl-1* and *unc-16* transcripts in dissected germlines of wild-type adult worms. Red – FISH probe. Blue – DAPI/DNA. Insets zoom in on pachytene germ cells. Scale bar: 20 μm.

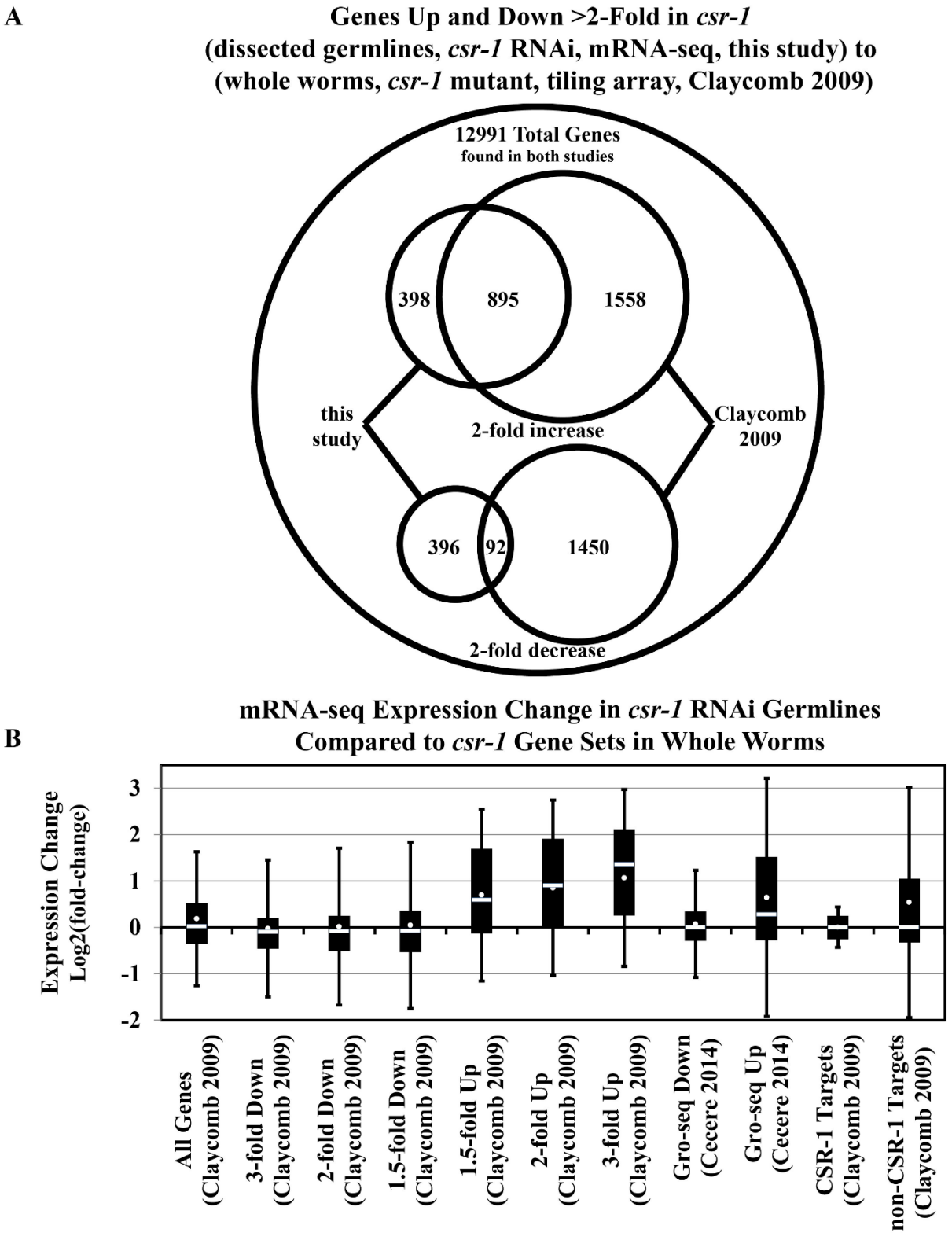

Figure S3. Comparison of *csr-1* RNAi germline expression to *csr-1* gene sets in whole worms. A) Genes up and down-regulated >twofold in dissected *csr-1* RNAi germlines (mRNA-seq, this study) compared to *csr-1* whole worms (tiling microarray, Claycomb 2009). B) Comparison of expression changes in *csr-1* RNAi germlines compared to *csr-1* gene sets in whole worms. Box, upper and lower quartiles; line, median; dot, mean; bars, standard deviation from mean.

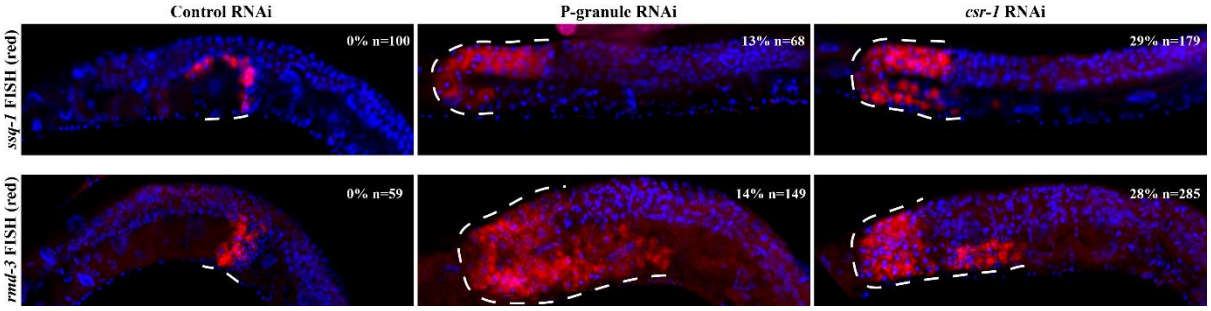

Figure S4. Distal expansion of *ssq-1* and *rmd-3* following P-granule and *csr-1* RNAi. Images show the left gonad arm in fixed, young adult worms. Expansion of expression is observed following either P-granule or *csr-1* RNAi. Red, FISH probe; blue, DAPI/DNA. Dashed line indicates domain of expression. The percentage of worms showing *ssq-1* and *rmd-3* expansion and the total number of worms examined are shown for each condition.

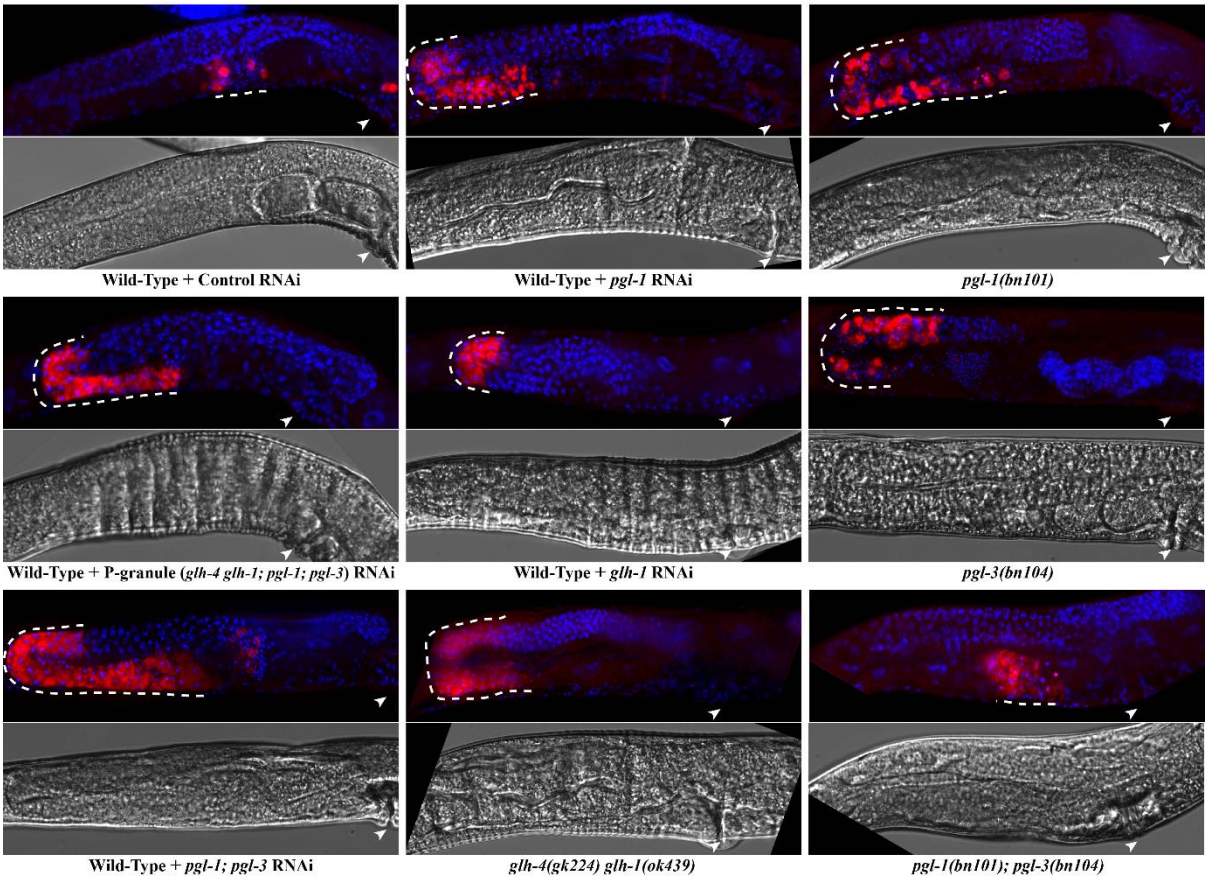

Figure S5. Distal expansion of *msp-3* transcripts when P granules are compromised. Images show the left gonad arm in fixed whole worms of day 1 adults. Ventral side down. Red, *msp-3* FISH probe; blue, DAPI/DNA. Dotted line indicates domain of *msp-3* expression. Arrowheads point to vulva.

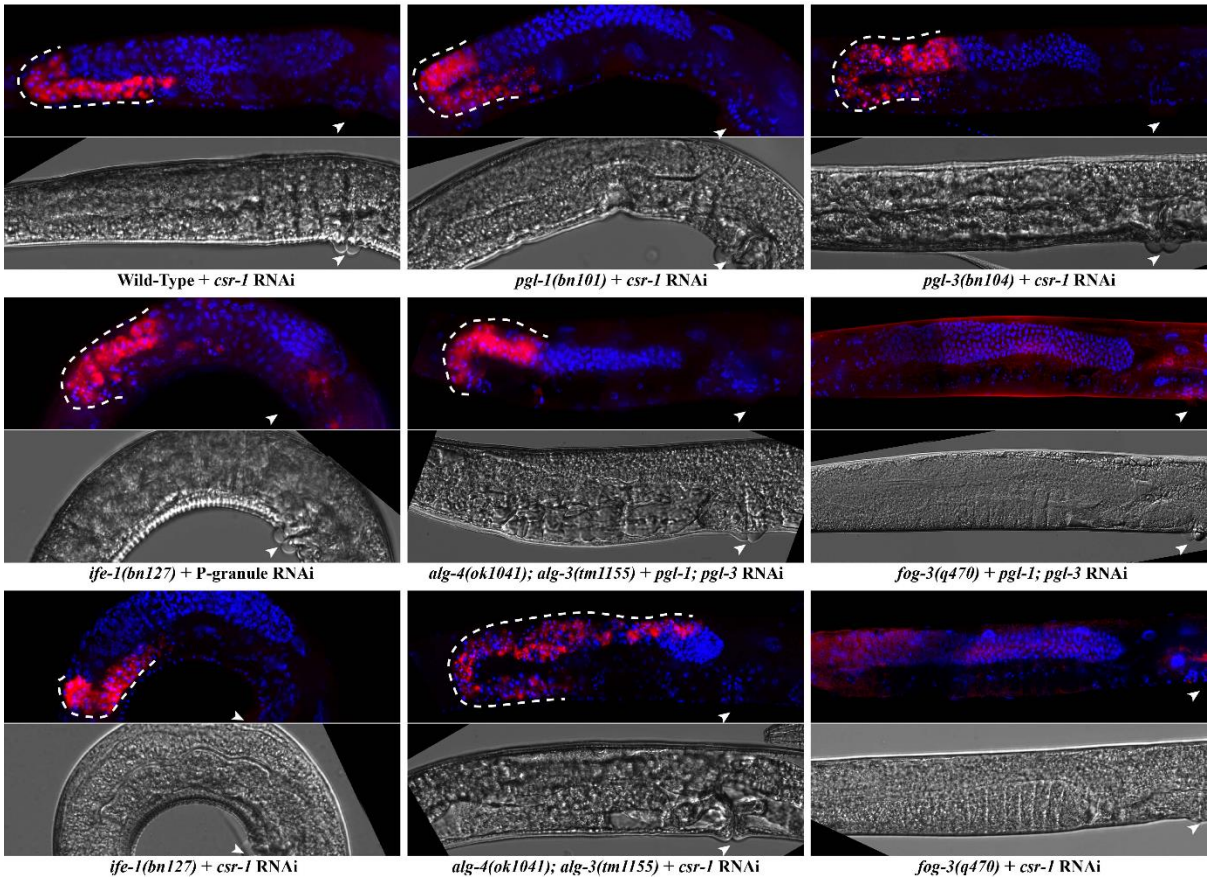

Figure S6. Distal expansion and suppression of *msp-3* expression. Images show the left gonad arm in fixed whole worms. Ventral side down. Red, *msp-3* FISH probe; blue, DAPI/DNA. Dotted line indicates domatin of *msp-3* expression. Arrowheads point to vulva.

Table S1. Interactive table used to compare P-granule and *csr-1* RNAi mRNA-seq germline expression changes. Column legend:

A) ID
B) Chromosome
C) Gene ID
D) Control RNAi – mean sequence counts (average of four replicates, normalized using DESeq)
E) P-granule RNAi – mean sequence counts (average of four replicates, normalized using DESeq)
F) P-granule RNAi – Log2 fold change compared to control.
G) p value – significance between the four control replicates to the four P-granule RNAi replicates
H) adjusted p value - calculated using the Benjamini-Hochberg method for multiple testing correction (Anders and Huber, 2010).
I) Set 1 genes – those genes differentially expressed following P-granule RNAi with a p value < 0.05
J) Set 2 genes – those genes differentially expressed following P-granule RNAi with an adjusted p value < 0.05
K) *csr-1* RNAi – mean sequence counts (average of four replicates, normalized using DESeq)
L) *csr-1* RNAi – Log2 fold change compared to control.
M) p value – significance between the four control replicates to the four *csr-1* RNAi replicates
N) adjusted p value - calculated using the Benjamini-Hochberg method for multiple testing correction (Anders and Huber, 2010).
O) Set 1 genes – those genes differentially expressed following *csr-1* RNAi with a p value < 0.05
P) Set 2 genes – those genes differentially expressed following *csr-1* RNAi with an adjusted p value < 0.05
Q) Germline enriched genes from (Reinke et al., 2004).
R) Germline enriched gender neutral. Column Q genes with gametogenesis genes depleted from (Reinke et al., 2004).
S) Soma enriched genes from (Reinke et al., 2004).
T) Neuron enriched genes from (Watson et al., 2008).
U) Spermatogenesis enriched genes from (Reinke et al., 2004).
V) Spermatogenesis enriched genes from (Ortiz et al., 2014).
W) List of genes encoding spermatogenesis proteins (Chu et al., 2006).

X) All spermatogenesis genes (sum of columns U, V, W)

Y) Oocyte enriched genes from (Reinke et al., 2004).

Z) Oocyte enriched genes from (Ortiz et al., 2014).

AA) Gene expression ratio in *csr-1* mutant tiling arrays from (Claycomb et al., 2009).

AB) Genes significantly upregulated by GRO-seq in *csr-1* hypomorphic mutants from (Cecere et al., 2014).

AC) Genes significantly down regulated by GRO-seq in *csr-1* hypomorphic mutants from (Cecere et al., 2014).

AD) Genes targeted by CSR-1-bound 22Gs identified in (Claycomb et al., 2009).

AE) Genes targeted by ALG-3/4-bound 26Gs identified in (Conine et al., 2013).

AF) Genes targeted by CSR-1-bound 22Gs in males, identified in (Conine et al., 2013).

Click here to Download Table S1